

Investigating the Microstructure and Mechanical Properties of Friction Stir Weld Joints of Solution Hardening Aluminium Alloy AA5086

Chaitanya Sharma*, D. K. Dwivedi, P. Kumar

Mechanical and Industrial Engineering Department, I.I.T. Roorkee, Uttarkhand, India-247667

*Corresponding author E-mail : chaitanya.sharmaji@gmail.com

ABSTRACT

Friction stir welding is one of the most suitable welding processes to join aluminum alloys, thanks to many economical and technical advantages associated with its use. This paper investigates effect of friction stir welding on the microstructure and mechanical properties of solid solution hardening Al-Mg-Mn aluminum alloy. Friction stir weld joints were developed using optimum combination of rotary speed and welding speed. The microstructure evolution in friction stir weld joints was studied by optical microscopy. Fine recrystallized grains were observed in weld nugget zone while thermo-mechanically affected zone showed distorted and unrecrystallized grains. Microhardness profiles and stress-strain curves were developed for friction stir weld joints and base material. Friction stir weld joints showed mechanical properties approximately equal to base material. Further, fracture surfaces were investigated using scanning electron microscope to study the mode of fracture.

Keywords: Friction stir welding, microstructure, mechanical properties, and solution hardening aluminum alloys.

1.0 INTRODUCTION

Aluminum and its alloys has gathered wide acceptance in the fabrication of lightweight structures for aviation, railway, marine and other sectors requiring a high strength to weight ratio, resistance to stress corrosion cracking etc than steels [1]. Several methods such as riveting, mechanical fastening and fusion welding, adhesive bonding are used to join aluminum and its alloys to fabricate structures [2]. Riveting produces stronger joints needs wider flange and add weight and distortion to the structure along with corrosion problem [3]. Though fusion welding techniques are routinely used for joining aluminum and its alloys, there are many difficulties associated with them such as cast dendritic microstructure, porosity, distortion, and cracking due to shrinkage in the weld metal and HAZ. Extensive softening results in the loss of strength in HAZ [4, 5]. These problems render aluminum

joining highly unattractive by riveting and fusion welding techniques.

Alternatively, aluminum and its alloys can be welded successfully by friction stir welding (FSW), a solid state welding process which is invented at the Welding Institute (TWI), Cambridge U.K. in 1991 [6]. FSW is the modification of conventional rotary friction welding processes used for joining cylindrical components. FSW relies on heat of deformation and friction between non consumable profiled tool and work piece for joining materials in solid state [7]. In FSW, shoulder and threaded pin of the rotating tool makes firm contact with the top surface and abutting edges of the work-piece respectively, when traversed along the weld line generates heat due to deformation of material and friction. Thus, work piece material is softened around the tool pin and transported from the advancing side to the retreating side of the joint where it is

consolidated into a joint due to dual action of extrusion and forging [8, 9]. As the peak temperatures observed during FSW are lower than melting temperature of the materials being joined, melting and solidification is absent in friction stir weld joint avoiding most of the problems of fusion welding of aluminum alloys [5, 10, and 11].

AA5086 is an Al-Mg-Mn alloy composed of a matrix of α Al (solid solution magnesium in aluminium), dispersion strengthened with fine precipitate of β phase Mg_2Al_3 . Manganese is added to improve the strengthening effect of the magnesium. High strength, light weight, good formability and cost effectiveness makes 5XXX and 6XXX series aluminum alloys a commonly used automotive structural material. Aluminum alloy AA5086 is a medium to high strength non-heat-treatable structural alloy, has good weldability, corrosion resistance and formability. As this alloy is resistant to stress corrosion cracking and exfoliation, it has wide range of applications in the marine, automotive, and aircraft parts, cryogenics, TV towers, drilling rigs, transportation equipment, missile components, gas & oil piping, ordnance & armor plate, and ship, boat & yacht hulls [12-14].

Literature review [15-22] reveals that considerable work has been reported on various aspects of friction stir welding of work hardening 1XXX and 5XXX series aluminum alloys. AA5083 is the most commonly friction stir welded aluminum alloy of 5XXX series with few studies on other 5XXX series aluminum alloys such as AA5086. Cam et al. [23] performed friction stir welding of AA5086 H-32 using a tool rotational speed of 1600 rpm and three different traverse speeds of 175, 200, and 225 mm/min and observed porosity and kissing bond defect at the root of the welds. Further, they concluded that strength and ductility of joints can be increased by optimizing welding speed and depth of tool penetration. Aval et al. [24] studied thermal cycle and temperature field generated during friction stir welding of AA5086 using mathematical models and found that temperature field in the FSW process is asymmetric. Peak temperatures were higher on the advancing side than the retreating side. Heat input strongly affected the microstructures of the joints. This research aims to study the microstructure and mechanical behavior of FSW joints of Aa5086.

2.0 EXPERIMENTAL WORK

The chemical composition as determined by Electron dispersive X-ray (EDAX) analysis of the as received AA 5086- O base material is presented in **Table 1**.

As received 6-mm thick rolled sheet was cut into pieces with the longer dimension in the rolling direction (RD) which were then machined on shaper to have size of 300 x 50 mm². These work pieces were held firmly in butt joint position using indigenously fabricated fixture. A single pass welding procedure was used to fabricate the joints from one side. FSW tool was made of hot die steel which was heat treated to 55 HRC. The truncated conical tool has flat shoulder of 17 mm diameter and cylindrical threaded pin of 8 mm top and 5 mm root diameters, 5.7 mm length. Pin has anticlockwise threads of 1 mm pitch. A constant tool tilt of 2.5° from the vertical axis was also used in order to facilitate the consolidation of plasticized material. Vertical Milling Machine (HMT India, 7 H.P.) was used to fabricate FSW joints. FSW parameters were optimized by making welds at constant rotary speed of 635 rpm and different welding speeds of 8, 19, and 30 mm/min. Subsequently welds were subjected to visual and destructive inspection to identify weld defects (if any) such as voids or tunnel defects. It was found that welds produced using welding speed of 8 and 19 mm/min showed tunnel defect and crack near exit hole one such weld joints is shown in **Fig 1**. Therefore, these joints were not investigated further. Weld joints produced using welding speed of 30 mm/min and rotary speed of 635 rpm were found sound and free from defects and their results are reported in this paper. After the FSW all the developed welds were subjected to visual inspection to identify detectable weld defects such as voids; groove or tunnel defects if any. In this way the analysis of flawed FSW joints can be avoided.

Tensile properties of FSW joints were evaluated immediately after fabrication. Joints were sliced using a power hacksaw and then conventional dumbbell shaped tensile specimens of 4 mm diameter and 25 mm gauge length were prepared as per the ASTM E8M-04 specification [25]. Tensile tests were carried out at a cross head speed of 1 mm/min using a 25 KN; electro-mechanically controlled universal testing machine (H25K-S,

Table 1 : Chemical Composition (wt %) of Base material

Al	Mg	Mn	Fe	Si	Cu	Ti	Zn	Cr
Bal.	4.11	0.51	0.12	0.09	0.01	0.04	0.02	0.02

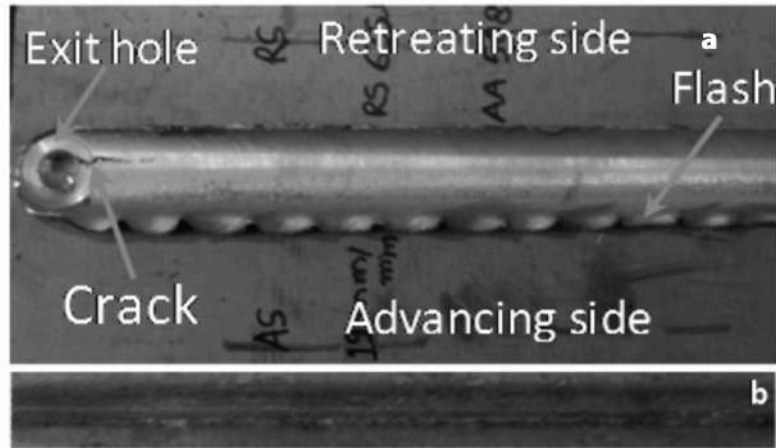


Fig. 1 : Friction stir weld Joint of AA 5086-O (a) Crown surface, (b) Root surface

Hounsfield). The 0.2% offset yield strength; ultimate tensile strength, and percentage elongation were recorded. Tensile tests were performed in triplicate and average values are presented for discussion. A Vickers microhardness tester (VHM-002V Walter UHL, Germany) was employed for measuring the hardness across the joint with a load of 100 grams and 30 seconds dwell time.

Microstructural analysis was carried out using a light optical microscope (Leica, Germany) on polished and etched specimens. Keller's reagent was used to etch the specimens (2ml nitric acid, 4ml hydrofluoric acid, and 94 ml water). A scanning electron microscope was used to characterize the modes of fracture of the tensile tested specimens.

3.0 RESULTS AND DISCUSSION

3.1 Microstructure

The macrostructure of the joints perpendicular to welding direction displaying different zones characteristic to FSW process is shown in Fig.2.

The frictional heat and extreme deformation caused by tool rotation and traversing lead to the formation of weld nugget zone (WNZ), thermo mechanically affected zone (TMAZ), and

heat affected zone (HAZ).The trapezoidal weld nugget had dimensions which closely matched with the shoulder and pin dimensions of the tool used. The top surface receives more heat and rejects less heat than the bottom surface of the plates. The differential thermal conditions experienced by top and bottom surfaces of the plates resulted in the widening of the weld nugget at the top and contraction of the same at the bottom [26].

Fig. 3 depicts the micrographs showing the microstructure of base material and FSW joints.

Base material (Fig. 3a) had randomly distributed large population of secondary strengthening intermetallic/dispersoid particles of varying size and shape. WNZ of FSW joints invariably showed equiaxed fine grain structure than the base material (Fig. 3 c) [15, 16]. The temperature in WNZ can be as high as 425 to 480°C during FSW and such high temperature are enough to cause dynamic recrystallization resulting in equiaxed fine grain structure than the base material [9-11]. The constituent $Al_3(Fe, Mn)_3Si$ and $Al_6(Fe, Mn)$ particles and submicron $Al_6(Fe, Mn)$ dispersoids present in the base material did not dissolve. These have been reported to dissolve at temperature about 635-700 °C [13, 14] higher than the peak temperature observed during FSW of aluminum

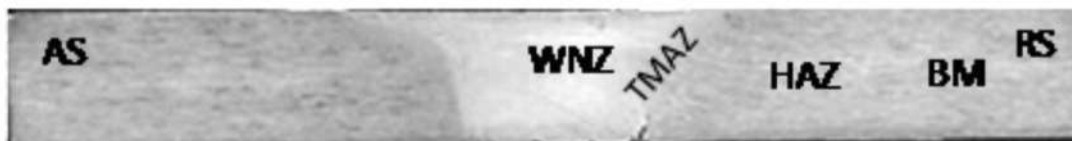


Fig. 2 : Macrostructure of joint showing the evolution of different FSW zones.

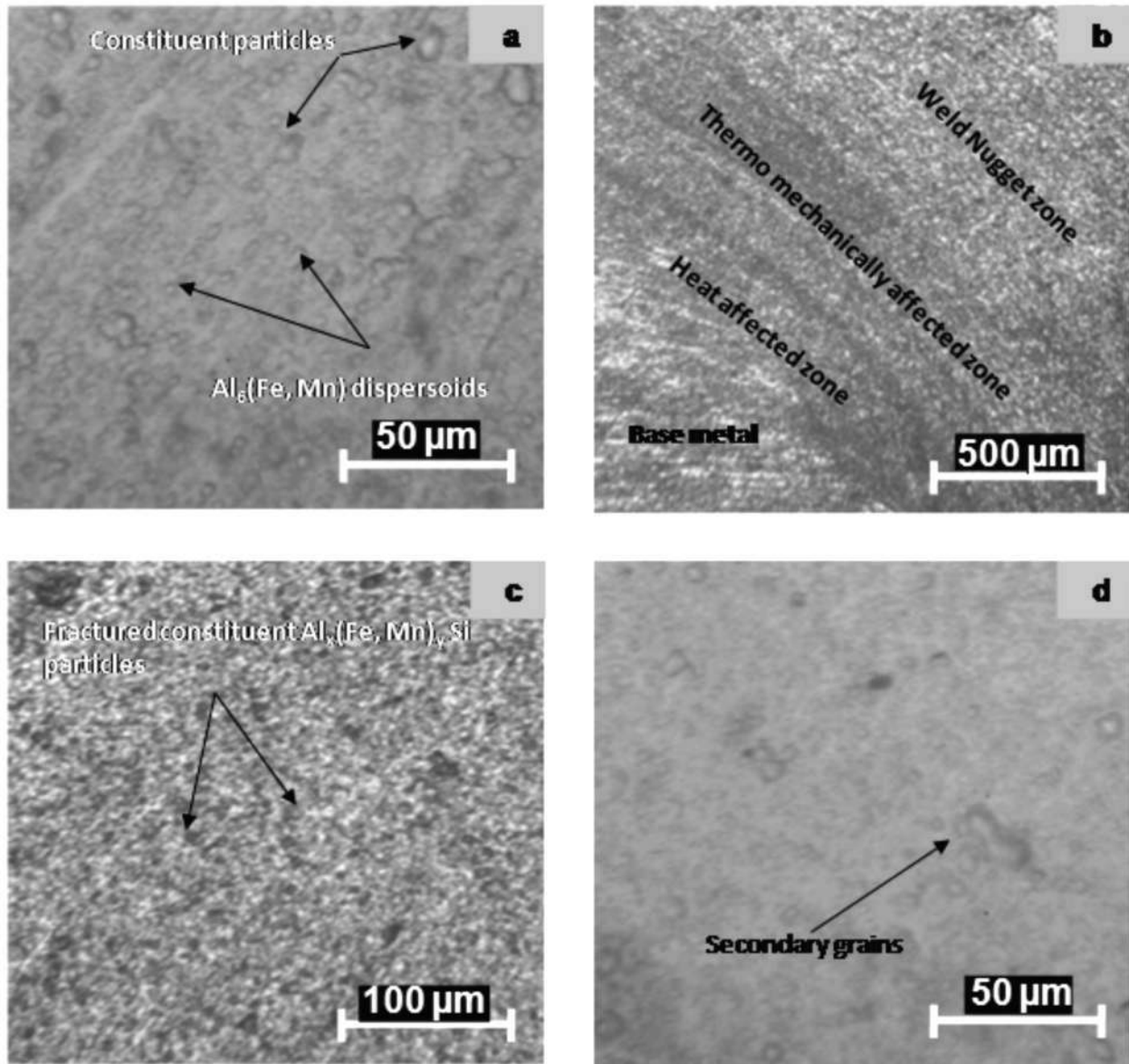


Fig. 3 : Microstructure of (a) Base material (b) Different FSW Zones Weld nugget, TMAZ and HAZ, (c) Fine recrystallized grains in weld nugget zone, and (d) Secondary grains in weld nugget zone.

alloys. Therefore, these constituent/intermetallic particles (dark in colour) experience only partial fracture/breakup due to tool stirring without dissolution during FSW as seen in **Fig. 3c** and **Fig. 3d**.

The TMAZ is a narrow region of highly deformed elongated and flattened non recrystallized grains. It was observed (**Fig. 3 b**) that microstructure of TMAZ contains severely deformed grains larger in size than WNZ grains. This may be attributed to the absence of dynamic recrystallization in TMAZ. In TMAZ, lower amount of frictional heating and plastic deformation could not initiate dynamic recrystallization because high stacking fault

energy of aluminum alloys acts as barrier to dynamic recrystallization [5, 9, and 10]. The WNZ and TMAZ interface is clearer on advancing side than retreating side (**Fig. 2**). This is attributed to higher plastic strains and shear flow stresses in narrow band on advancing side than other side where tool rotation add to pin translation [27] arising from the arrangement of directions of tool rotation and traversing. The region adjacent to TMAZ and outside the tool shoulder is the HAZ and had coarse grain structure than the base material (**Fig. 3 b**) In HAZ material is only affected by heat generated by friction between material and tool.

3.2 Microhardness

The hardness across the weld cross section in transverse direction of the FSW joints was measured by Vickers micro hardness tester. The recorded microhardness profiles for base material as well as for welded joints of AA5086 aluminum alloy are shown in **Fig. 4**.

The microhardness profile is relatively flat and does not has distinct hardness maxima as usually observed for peak hardened heat treatable aluminum alloys. Microhardness profile is slightly asymmetrical with respect to the weld center line because of non uniform field of plastic flow [9, 26]. The average micro hardness of unwelded base material is 76 H_v. The average microhardness of weld nugget is 77.9 H_v, slightly higher than base material. The minimum hardness of 51 H_v is obtained in HAZ and maximum hardness of 84 H_v, is obtained in weld nugget on retreating side (RS) of the joints. Thus variations in the hardness of friction stir welded joints are very small (+1.8 to -8.5 HV), which is the expected response from a fully annealed work hardenable aluminium alloy. According to Hall–Petch relationship hardness is the reciprocal of the square root of grain size [20]. Thus smaller is the grain size higher will be the hardness of materials or vice versa. It is well known that FSW refines microstructure of base metal and produces fine

recrystallized grains of the order of 1-15 μm in WNZ [5, 10 and 26]. This fine recrystallized grain structure is responsible for the higher hardness of WNZ than base metal [20]. Additionally, strain hardening of annealed base metal due to intensive plastic deformation during FSW also increases hardness of FSW joints [27]. Similar trends of results were reported by Sato and Karlsson [20, 21] for FSW joints of AA5083-O aluminum alloy.

3.3 Tensile properties

Tensile properties of defect free FSW joint were measured by conducting traverse tensile tests. **Table 2** represents the average tensile properties of friction stir welds as well as of base material for comparison.

Engineering stress and strain diagrams for base metal and as welded friction stir welds are presented in **Fig. 5**. From strain stress curve it is evident that FSW joints had improved % elongation and deteriorated tensile yield and ultimate strength (Refer table 2).

FSW results in no appreciable change in ultimate tensile strength while yield strength falls considerably. Yield and ultimate tensile strength of FSW joints was found to be 23.2 and 1.8% lower and percentage elongation 19.3 % higher than

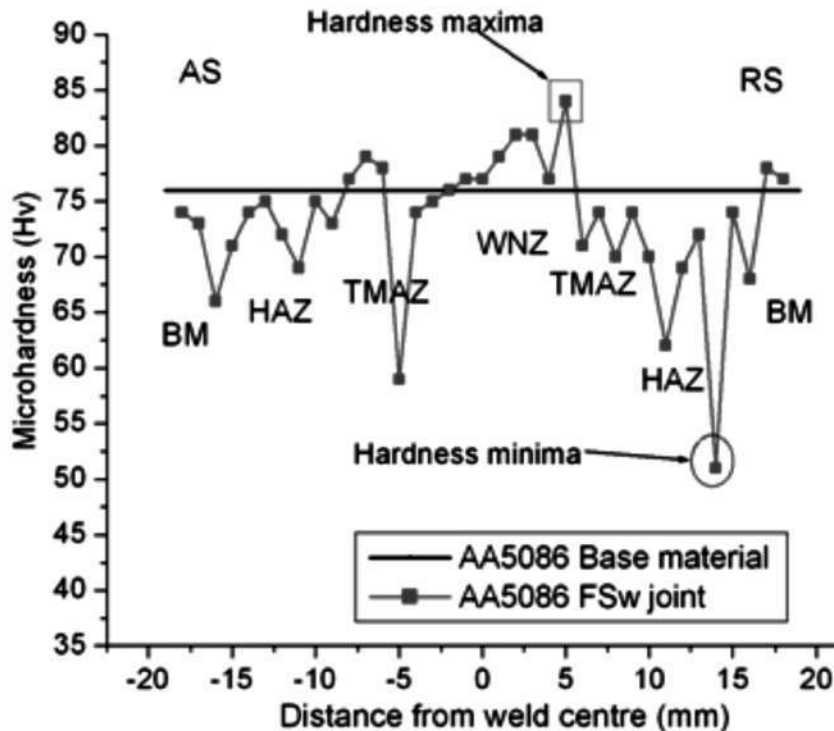


Fig. 4 : Microhardness profile of FSW joint and base material of AA5086

the base material. FSW drastically increased percentage elongation of welds from 21.2 to 25.3% approximately by 19.3%. The nearly equal ultimate tensile strength and higher % elongation of the FSW joints than base metal may be attributed to grain refinement on account of dynamic recrystallization [15]. Dynamic recrystallization resulted in the formation of strain free soft recrystallized grains in the weld nugget zone and tool stirring causes partial fracture/breakup of coarse constituent/intermetallic particles. These factors are supposed to reduce stress localization which in turn resulted in better tensile properties of FSW joints

The ratio of weld strength to base material strength is defined as the joint efficiency. Accordingly ultimate tensile strength efficiency, yield strength efficiency and elongation efficiency of friction stir welded joints of AA5086 aluminum alloy were 98.2 %, 76.8 % and 119.3 %. Uematsu et al. [28] reported 100 % joint efficiency for AA5083 welded in annealed condition and attributed same to strengthened weld nugget by grain refinement.

The tensile properties of defect free sound FSW joints are governed by microhardness distribution across the joint. During tensile testing the samples fractured through minimum hardness region of HAZ having lower tensile strength on retreating side along a path inclined at 45° to the axis of loading which correspond to minimum hardness contour. Threadgil et al. [29] reported that when solid solution treated aluminum alloys welded in annealed condition failure of cross weld joint during tensile test can occur anywhere on the specimen but it usually occur in base metal away from the weld. **Fig. 6** displays fractured tensile specimen.

3.4 Fracture Surfaces

Scanning Electron Microscope was used to study the modes of failure of the tensile test specimens. SEM micrographs of FSW joints are shown in **Fig 7**.

Low magnification SEM fractographs (**Fig.7 a**) shows whole fracture surface which is covered with dimples and some featureless flat regions are also visible. The presence of

Table 2 : Tensile properties of friction stir weld joints and base material

Material condition	Ultimate tensile strength	Yield strength (MPa)	Elongation (%)	TSE (%)	YSE (%)	EE (%)
Base Metal	294.8	203.7	21.2	-	-	-
As welded	289.6	156.4	25.3	98.2	76.8	119.3

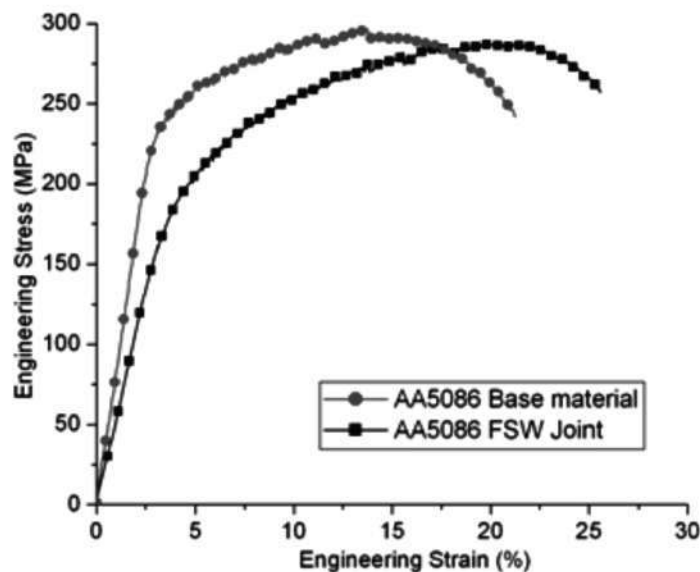


Fig. 5: Engineering stress and strain diagrams for base metal and FSW joints

dimples is an indication of locally ductile fracture [30]. At higher magnification fracture surface is full of dimples of varying sizes and shapes. Some deep and elongated dimples are also present along with tear ridges on the fracture surface (**Fig 7 b**). These deep and elongated dimples require larger mechanical deformation prior to failure, resulting in ductile fracture while presence of tear ridge reflects materials ability to sustain the tensile load after microvoid coalescence has begun [10]. The marked dimpled area A and flat area B were further analyzed at higher magnification. The hard and brittle intermetallic particles initiate the void formation which grows in size with the continuing deformation. When these particles fail to maintain the compatibility of deformation they get fractured leading to failure of the specimen. The closer examination of flat region B reveals the presence of shallow and deep dimples which were sheared off during fracture of the joint. As the percentage elongation is more than the base material by 19.3% it seems that the fracture is governed by ductile mode.

4.0 CONCLUSIONS

Al-Mg-Mn alloy AA5086 is readily weldable by FSW process with properties nearly equal to base material. FSW transformed the microstructure of base material and creates WNZ, TMAZ and HAZ in the base material. Fine grained recrystallized microstructure in WNZ is mainly responsible for higher hardness of WNZ than base material. The decrease in yield strength of friction stir weld joints was more serious than decrease in ultimate tensile strength. Based on the findings of this research, it is recommended that friction stir welding of AA5086 should be performed in annealed condition to obtain joints with base metal properties i.e. to minimize the loss of mechanical properties.

REFERENCES

1. Cam, G. and Kocak, M. (2007); Microstructural and mechanical characterization of electron beam welded Al-alloy 7020, *Journal of Material Science*, 42, pp. 7154–7161.
2. Jariyaboon M., Davenport A. J., Ambat R., Connolly B. J., Williams S. W. and Price D. A. (2009); The effect of cryogenic cooling on corrosion behavior of friction stir welded AA2024-T351, *Corrosion Engineering Science and Technology*, 44, pp. 425-432.
3. Williams S. W. (2001); Welding of airframes using friction stir, *Air and Space Europe*, 3 (3-4), pp. 64-66.
4. Dawes C. J., Thomas W. M. FSW welds of aluminum alloys. (1996); The process produces low-distortion, high-quality, low-cost welds on aluminum, *Welding Journal*, 75, pp. 41-45.
5. Hassan, Kh. A. A., Prangnell, P. B., Norman, A. F., Price, D. A. and Williams, S. W. (2003); Effect of welding parameters on nugget zone microstructure and properties in high strength aluminium alloy friction stir welds, *Science and Technology of Welding and Joining*, 8(4), pp. 257–268.
6. Thomas W. M., Nicholas E. D., Needham J. C., Nurch M. G., Smith P. and Dawes C. J. (1991); Friction stir butt welding, International Patent Application No. PCT/GB92/02203.
7. Nandan R., Deb Roy T. and Bhadeshia H. K. D. H. (2008); Recent advances in friction stir welding-Process, weldment structure and properties, *Progress in Materials Science*, 53 (6), pp. 980-1023.



Fig. 6 : Fractured tensile specimens of FSW joints

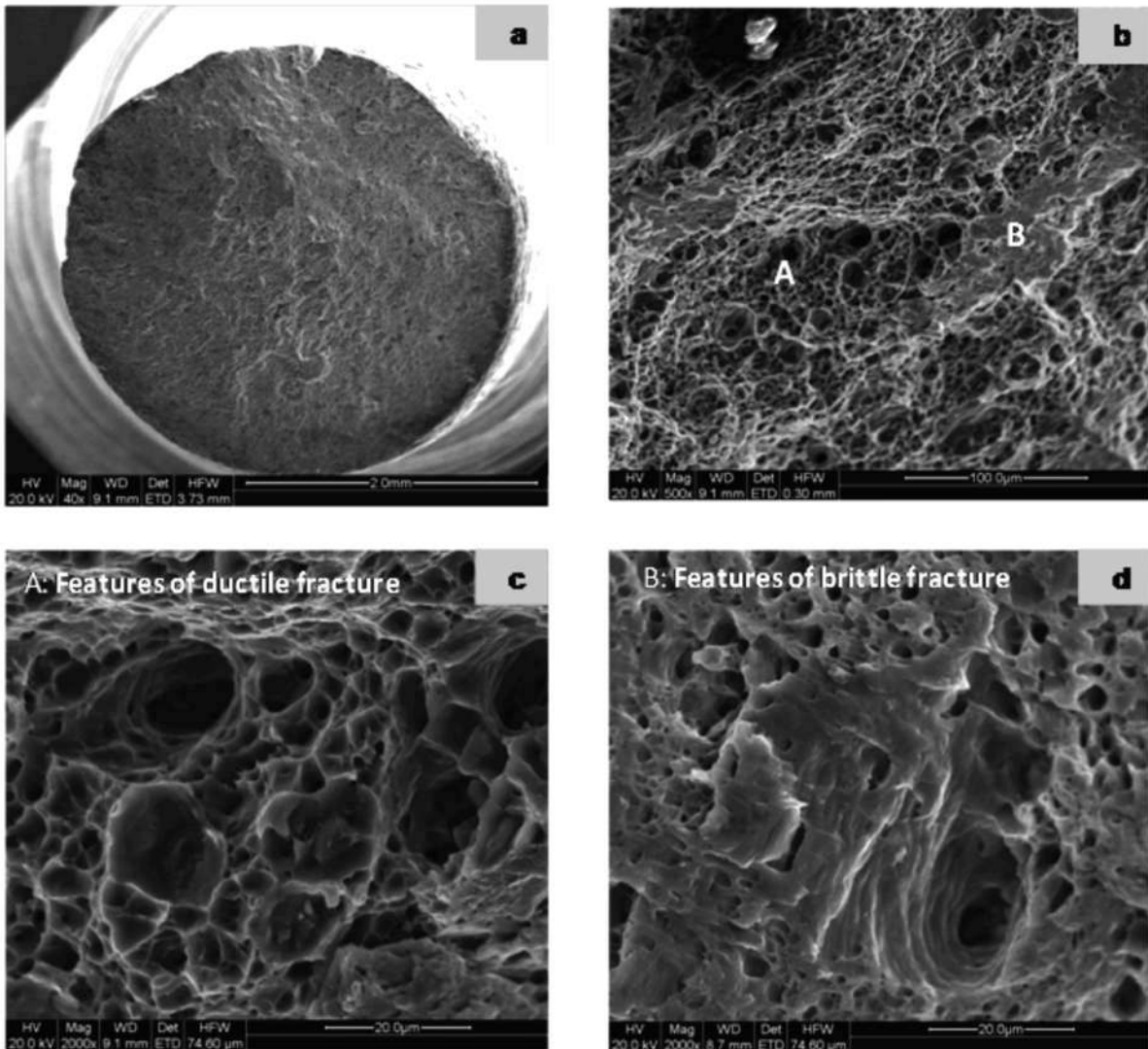


Fig. 7 : Fractographs of tensile tested FSW joints

8. Siedel T. U. and Reynolds A. P. (2001); Visualization of the material flow in AA2295 friction stir welds using marker insert technique, *Metallurgical and Materials Transactions A*, 32, pp. 2879-2884.
9. Zhang Z., Zhang H. W. (2009); Numerical studies on controlling of process parameters in friction stir welding, *Journal of Materials Processing Technology*, 209, pp. 241-270.
10. Mahoney, M. W., Rhodes, C. G., Flintoff J. G., Spurling, R. A., and Bingel, W. H. (1998); Properties of friction stir welded 7075 T651 aluminum, *Metallurgical and Materials Transactions A*, 29, pp. 1955-1964.
11. Rhodes C.G., Mahoney M. W., Bingel W. H., Spurling R. A., Bampton C. C., (1997); Effects of friction stir welding on microstructure of 7075 aluminium, *Scripta Materialia*, 36, pp. 69-75.
12. ASM Handbook Vol. 2, (1992); Properties and Selection: Nonferrous Alloy and Special Purpose Materials, pp. 364-367.
13. Hatch J. E. (1984); *Aluminum: Properties and physical metallurgy*, American society for metals, USA.
14. Polmear I. J. (1995); *Light alloys: metallurgy of light metals*, St. Edmundsbury press Ltd., Bristol UK.
15. Peel M., Steuwer A., Preuss M. and Withers P. J. (2003); Microstructure, mechanical properties and residual stresses as a function of welding speed in AA5083 friction stir Welds, *Acta Materialia*, 51, pp. 4791-4801.

16. Hong S., Kim S., Lee C. G and Kim S. J. (2007); Fatigue crack propagation behavior of friction stir welded 5083-H32 aluminum alloy, *Journal of Materials Science*, 42, pp. 9888-9893.
17. Zhou C., Yang X. and Luan G. (2006); Effect of oxide array on fatigue property of friction stir welding, *Scripta Materialia* 54, pp. 1515-1520.
18. Frankel G., and Xia Z. (1999); Localised corrosion and stress corrosion cracking resistance of friction stir welded aluminium alloy 5454, *Corrosion* 55(2), pp. 139-150.
19. Lim, et al., (2005); Mechanical Properties of FSW aluminium Alloys with Different Hardening Mechanisms. *Metals and Materials International*, 11(2), pp. 113-120.
20. Sato Y., Hwan S., Park C. and Kokawa H. (2001); Microstructural factors governing hardness in friction stir welds of solid solution hardened aluminum alloy. *Metallurgical and Materials Transactions A*, 32, pp. 3033-3042.
21. Karlsson et al., (1999); Characteristics of FSW aluminium alloys, *Proceedings of Fifth International Conference. ASM International*, pp. 574-579.
22. Zhou C., Yang X. (2006); Effect of kissing bond on fatigue behavior of friction stir welds on Al 5083 alloy, *Journal of Material Science*, 41, pp. 2771-2777.
23. Çam G., Güçlüer S. A., Çakan A., Serindağ H. T. (2008). Mechanical properties of friction stir butt-welded Al-5086 H32 plate. *Journal of Achievements in Materials and Manufacturing Engineering*, 30, pp. 151-156.
24. Aval H. J, Serajzadeh S, Kokabi A. H. (2011). Theoretical and experimental investigation into friction stir welding of AA 5086. *International Journal of Advance Manufacturing and Technology*, 52, pp. 531-544.
25. ASTM E8/E8M-09. (2009); ASTM International, Pennsylvania United States.
26. Sharma, C., Dwivedi, D. K., and Kumar, P. (2012); Effect of welding parameters on microstructure and mechanical properties of friction stir welded joints of AA7039 aluminium alloy, *Materials Design* 36, pp. 379-390.
27. Cabibbo M., McQueen H. J., Evangelista E., Spigarelli S., Di Paola M. and Falchero A. (2007); Microstructure and mechanical property studies of AA6056 of friction stir welded plate. *Material Science and Engineering A*, 460-461, pp. 86-94.
28. Uemastu Y., Tokaji K., Shibata H., Tozaki Y. and Ohmune T. (2009); Fatigue behavior of friction stir welds without neither welding flash nor flaw in several aluminum alloys. *International Journal of Fatigue*, 31(10), pp. 1443-1453.
29. Threadgill P. L., Leonard A. J., Sherdiff H. R. and Withers P. J. (2009) Friction stir welding of aluminium alloys. *International Materials Reviews*, 54 (2), pp. 49-93.
30. Sharma, C., Dwivedi, D. K., and Kumar, P. (2012); Influence of In-process cooling on tensile behavior of FS Wed joints of AA7039, *Material Science and Engineering A*, 556 (10), pp. 479-487.